Wideband Co-Linearly Polarized Microstrip Antenna for In-Band Full-Duplex Systems Using Two Parallel L-Probes

Yongkang Peng, *Graduate Student Member, IEEE*, Jiangwei Sui, *Member, IEEE*, Du Li, *Member, IEEE*, Junru Li, *Member, IEEE*, and Xiangwei Zhu, *Member, IEEE*

***Abstract*—A co-linearly polarized wideband microstrip antenna with a single shared patch feeding by two parallel L-probes is proposed in this letter. The shared patch introduces a new coupling path for the L-probes. The coupling coefficients of the two L-probes, as well as the L-probe and the patch, are quantitatively derived based on the coupled resonators theory. It is proved that by adjusting the geometries and dimensions of the two L-probes and the patch, a natural wideband high isolation can be obtained. A demonstration example is designed and measured to validate the feasibility of the proposed scheme. The results show that the proposed antenna can achieve impedance matching of −10 dB and high isolation of 20 dB in the frequency range from 3.2 GHz to 4 GHz. Besides, the measured efficiency ranges from 91% to 99% with an average realized gain of 7.4 dB. Furthermore, another example with a lower height is also designed to justify the practical usefulness, showing 19.8% decoupling bandwidth.**

***Index Terms*—Copolarized, full-duplex antennas, L-probe, microstrip antenna, shared patch, wideband.**

I. Introduction

The in-band full-duplex (IBFD) is believed to be a promising solution to provide higher data rates in modern and future wireless communication [1], [2]. A main challenge for successful IBFD is the self-interference cancellation (SIC), which mainly contains three parts: the antenna domain, the analog domain, and the digital domain, and a good antenna domain SIC will ease the burden of the subsequent two SICs and reduce the design complexity and cost of the whole system.

A straightforward method to achieve antenna domain SIC is to separate the transmitting (TX) and receiving (RX) antennas with a large distance [3], which is simple but occupies a bulky size. Some decoupling structures have been proven to be effective in improving antenna isolation, such as defected ground structures (DGSs) [4], metamaterial [5], parasitic decoupling elements [6], [7]; antenna decoupling surface (ADS) [8], [9]; sequential feeding networks [10], [11], [12]; and so on. To further reduce the size and complexity, the self-decoupling concept has been proposed, including using the weak-field area [13], the characteristic mode [14], hybrid mode superposition [15], [16], [17], coupling cancellation [18], [19], mode cancellation [20], and high order modes [21]. Although no extra decoupling structures are required, the TX and RX antennas in all these methods are still two separate radiators.

In recent years, the shared antenna for IBFD applications has become more and more attractive because of its compact size and easy integration into the monostatic system. The dual-polarized IBFD antennas can inherently obtain high isolation because of the orthogonal polarizations [22], [23]. To further improve the throughput, the copolarized IBFD antennas without costing the polarization resource are drawing great attention. First, the central shared part between two co-located ME dipoles can be modified to obtain natural high isolation for co-linearly polarized IBFD applications [24]. The grounded coupling pins [25], and a hybrid structure of slot and capacitor [26], also prove effective in tuning the common mode impedance to mitigate that of the differential mode. By exploring a fence-strip resonator [27] or chip capacitors with metallic vias [28], the radiating current is confined in the half part of the patch so that mutual coupling is naturally suppressed. Besides, two out-of-phase TM_{10} modes are generated to support the copolarized high isolation [29] with an additional conducting block to enhance the decoupling depth. However, these methods all focus on the decoupling of narrow bandwidth for 20 dB isolation. In [30], a four-port microstrip antenna design realized 16.2% isolation bandwidth using modes combination but suffers a large patch size of approximately 1.5λ × 2.5λ. Very recently, a wideband copolarized microstrip antenna has been proposed based on mode cancellation at the cost of an extra stacked patch [31]. Therefore, wideband co-linearly polarized IBFD microstrip antenna using one single patch is challenging and worthy to be investigated.

In this letter, a wideband co-linearly polarized IBFD microstrip antenna using two parallel feeding L-probes is presented. The shared patch introduces a second coupling path between the two probes, which is exactly counteracted by the original one naturally. Furthermore, due to the wideband feature of the L-probe feeding structure [32], [33], a wide bandwidth is naturally achieved. Compared with the existing works, there are mainly three distinct contributions.

1) It achieves inherent high isolation using the same radiating patch without using extra decoupling structures.

Received 3 August 2024; revised 4 September 2024; accepted 9 September 2024. Date of publication 12 September 2024; date of current version 13 December 2024. This work was supported in part by the National Key R&D Program of China under Grant 2021YFA0716500; in part by the National Natural Science Foundation of China under Grant 62201625; and in part by Guangdong Basic and Applied Basic Research Foundation under Grant 2021A1515110728. *(Corresponding author: Jiangwei Sui.)*

The authors are with the School of Electronics and Communication Engineering, Shenzhen Campus of Sun Yat-sen University, Shenzhen 518000, China (e-mail: pengyk3@mail2.sysu.edu.cn; suijw@mail.sysu.edu.cn; lidu5@mail.sysu.edu.cn; lijr85@mail.sysu.edu.cn; zhuxw666@mail.sysu.edu.cn).

Digital Object Identifier 10.1109/LAWP.2024.3459388

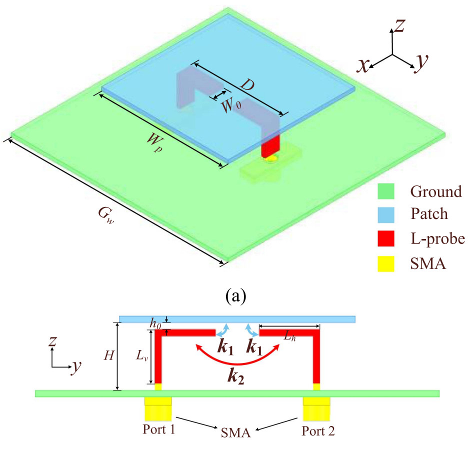

Fig. 1. Geometry of the proposed patch-shared IBFD microstrip antenna. (a) Perspective view. (b) Side view. G_w = 120 mm, W_p = 35 mm, D = 22.5 mm, W_0 = 7 mm, H = 15 mm, L_v = 12.5 mm, L_h = 6 mm, and h_0 = 1.5 mm.

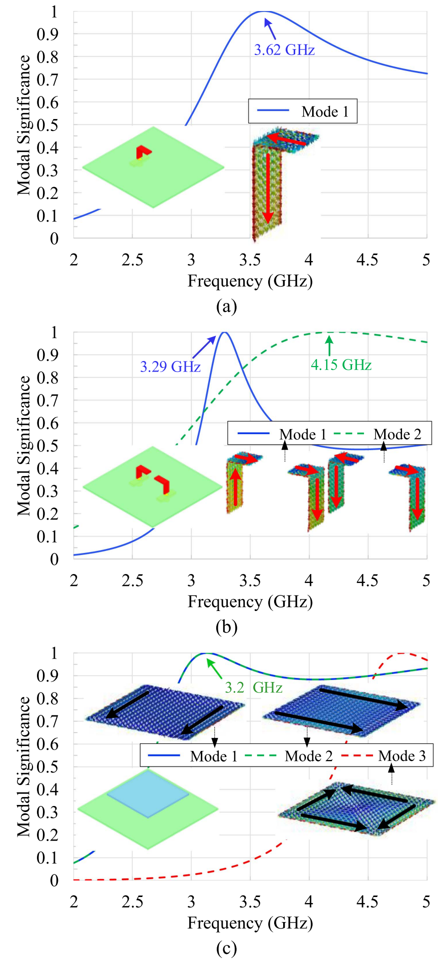

Fig. 2. Simulated modal significances and current distributions. (a) Single L-probe. (b) Two coupled L-probes. (c) Single square patch.

2) It achieves a wide matching and isolation fractional bandwidth of about 22%, benefiting from the natural L-probe feeding.
3) The coupling coefficients are analytically derived based on the coupled resonators theory.

II. Working Mechanism

As illustrated in Fig. 1, the proposed air-filled patch-shared microstrip IBFD antenna consists of a shared radiating patch, two L-probe feeding structures, a ground plane, and two SMA connectors, with detailed dimensions listed in the figure caption.

The coupling coefficients of the probe-patch and probe-probe are investigated in this part. The coefficients of these two kinds of coupling are defined as k_1 and k_2, respectively, as shown in Fig. 1(b). In the probe-patch-probe path, the energy from the excited probe is coupled twice to the coupled probe, so the total coupling coefficient of this path is ${k_1}^2$. To mitigate the coupled energy in the coupled probe, these two coefficients should satisfy the formula as follows:

$$-k_2 = k_1^2. \tag{1}$$

According to the classical coupled resonators theory, when two resonators are coupled, the original characteristic resonant frequency f_{01} and f_{02} will turn into two new resonances of f_l and f_h, and the coupling coefficient k of the two coupled resonators can be calculated using the formula as follows [34], [35]:

$$|k| = \frac{1}{2}\left(\frac{f_{02}}{f_{01}} + \frac{f_{01}}{f_{02}}\right)\sqrt{\left(\frac{f_h^2 - f_l^2}{f_h^2 + f_l^2}\right)^2 - \left(\frac{f_{02}^2 - f_{01}^2}{f_{02}^2 + f_{01}^2}\right)^2}. \tag{2}$$

When the two resonators are identical, it will be simplified into the following form:

$$|k| = \frac{f_h^2 - f_l^2}{f_h^2 + f_l^2}. \tag{3}$$

Fig. 2 shows the simulated modal significances using the characteristic mode analysis method. As shown in Fig. 2(a), the quarter-wavelength L-probe resonates at f_{01} = 3.62 GHz. After introducing another L-probe as depicted in Fig. 2(b), the original mode of a single L-probe splits into two modes, with one odd mode resonating at 3.29 GHz and the other even mode resonating at 4.15 GHz. Therefore, the coupling coefficient k_2 can be readily calculated by substituting f_l = 3.29 GHz and f_h = 4.15 GHz into (3), leading to $|k_2| = 0.228$. Considering the capacitive feature of k_2, it is easy to find that $k_2 = -0.228$.

In the case of a single square patch in Fig. 2(c), only the lowest three dominant modes are presented, where those of TM_{10} mode and TM_{01} mode resonating at f_{02} = 3.2 GHz overlap due to the square dimension of the patch. It's observed in Fig. 3(a) that in the case consisting of an L-probe and a patch, there are mainly 4 modes in the band of 2 GHz to 5 GHz, and modes 1 and 3 of Fig. 2(c) almost remain unchanged as modes 2 and 4 in L-probe-fed antenna's modes of Fig. 3, which means that for these two modes, there is nearly no coupling between the patch and the L-probe. Differently, for the characteristic modes 1 and 3 in Fig. 3, there are obvious coupled currents in the patch and the L-probe, showing effective coupling between these two antenna resonators. Therefore, combining the original resonances of f_{01} and f_{02}, the coupling coefficient k_1 can be calculated with f_l = 2.39 GHz and f_h = 3.81 GHz using the general formula (3), which is found to be −0.421 so that the coupling coefficient of the probe-patch-probe path, ${k_1}^2$, is equal to 0.177. As can

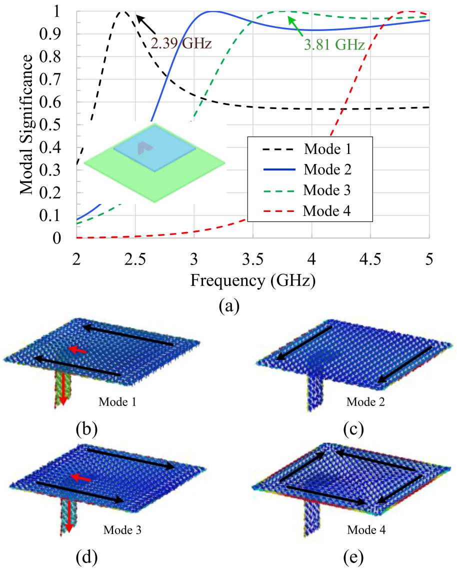

Fig. 3. Simulated modal significances and current distributions for an L-probe-fed patch antenna. (a) Modal significances. (b)–(e) Current distributions of the four dominant characteristic modes.

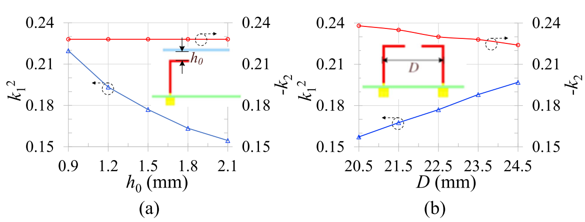

Fig. 4. Coupling coefficients with different relative distances. (a) h_0 of the patch and the probe. (b) D of the probes.

be seen, there is little difference between $-k_2$ (0.228) and $k_1{}^2$ (0.177) so Formula (1) can be roughly met, meaning the signal from the probe-probe path can be well mitigated with that from the probe-patch-probe path, leading to the inherent self-decoupling.

In a specific design, the coupling coefficients can be readily manipulated by tuning the dimensions of the patch and the L-probes. Without loss of generality, two key parameters, the gap between the patch and the L-probe h_0 and the separation of the two L-probes D are studied. As is shown in Fig. 4(a), when h_0 changes, the coupling coefficient $k_1{}^2$ can be tuned effectively, while k_2 maintains the same since the relative distance and dimensions of the two L-probes do not change. Besides, the coupling coefficients $k_1{}^2$ and k_2 can be tuned simultaneously by changing the parameter D. The S-parameters versus different values of h_0 and D are shown in Fig. 5. It can be seen that, with the increase of h_0, the S_{11} moves to the higher band greatly and the isolation is moved to the lower band. Besides, by increasing the relative distance D, the isolation minimum point moves to the higher band while S_{11} changes slightly.

One thing that should be mentioned is the wide impedance matching is obtained mainly benefiting from the L-probe feeding structure but not from the high profile of the patch.

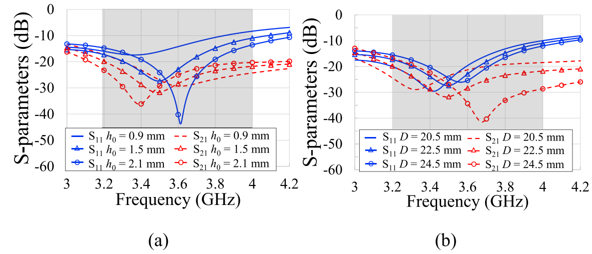

Fig. 5. S-parameters versus different relative distances. (a) h_0. (b) D.

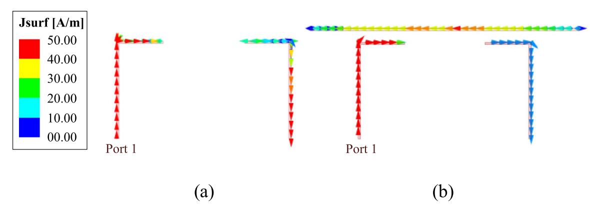

Fig. 6. Simulated current distributions. (a) Without shared patch. (b) With shared patch.

Fig. 7. Photographs of the fabricated copolarized patch-shared microstrip IBFD antenna. (a) Top view. (b) Side view.

III. Results and Discussions

A. Current Distributions

To observe the decoupling principle more clearly, Fig. 6 shows the simulated surface current distributions without and with the shared patch at 3.5 GHz, respectively. Only port 1 is excited in both cases. It is observed that the excited probe can excite the out-of-phase current on the coupled probe and the patch. When the out-of-phase current on the patch is coupled to the coupled probe, the coupled current through this path will be in-phase. Therefore, in Fig. 6(b), the addition of the patch introduces the probe-patch-probe coupling path, which counteracts the original probe-probe coupling path, making the current magnitude at the coupled probe close to nearly zero.

B. Fabrication and Measurement

The top and side view of the fabricated prototype are shown in Fig. 7. The patch and L-probes are 0.3 mm-thick copper and that is 0.5 mm for the ground. The simulated and measured S-parameters of the prototype antenna are illustrated in Fig. 8, in which the two results coincide well with each other. In the frequency range from 3.2 GHz to 4 GHz, the isolation is better than 20 dB, while S_{11} is better than -10 dB, demonstrating a 22.2% fractional bandwidth.

Fig. 9 demonstrates the measured gain and total efficiency of the proposed antenna, with a photograph of the experimental

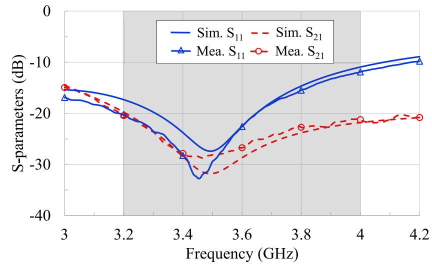

Fig. 8. Simulated and measured *S*-parameters of the proposed patch-shared microstrip IBFD antenna.

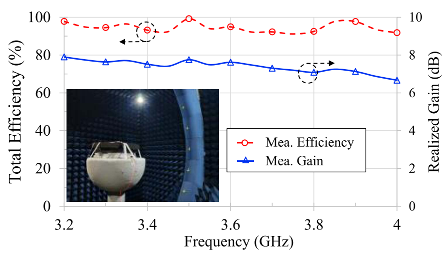

Fig. 9. Measured total efficiency and gain of the proposed patch-shared microstrip IBFD antenna.

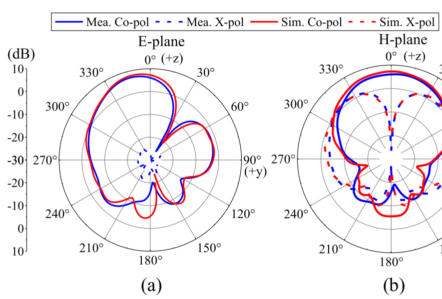

Fig. 10. Simulated and measured radiation patterns of the proposed patch-shared microstrip IBFD antenna at 3.5 GHz. (a) E-plane. (b) H-plane.

environment inserted. It can be found that the average efficiency reaches 94% in the band from 3.2 GHz to 4 GHz. Besides, the realized total gain is more than 6.7 dB in the operating band, with an average gain of 7.4 dB. Fig. 10 shows the simulated and measured radiation patterns of the prototype in the E-plane and H-plane at 3.5 GHz. It can be seen that the measured results are consistent with the simulated ones except for the cross-polarization of the E-plane, which is caused by the slight asymmetry introduced by the L-probe soldering error. Moreover, in the broadside radiation direction, the cross-polarization level of both the E-plane and H-plane is lower than -26.7 dB. To justify that the proposed antenna can also be applied for MIMO applications, the envelope correlation coefficient (ECC) is also studied, which is lower than 0.001 across the operating band of 3.2 GHz to 4 GHz, showing a very low spatial correlation.

To demonstrate the practical usefulness, another example working in the band of 3.27 GHz to 3.99 GHz is designed with the antenna height reduced from 15 mm to 10 mm. As can be seen in Fig. 11, although with a lower height, the proposed antenna achieves approximately 20% decoupling bandwidth with isolation better than 20 dB and S_{11} greater than -10 dB.

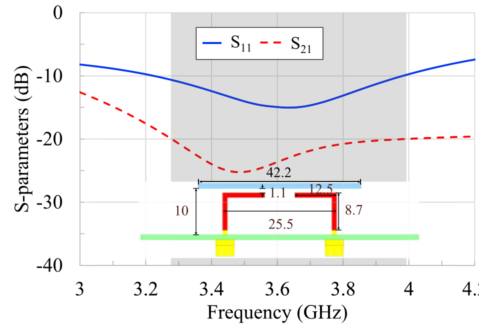

Fig. 11. Simulated *S*-parameters of the antenna with a height of H = 10 mm. The unit used here is mm.

TABLE I
COMPARISONS OF SOME STATE-OF-THE-ART HIGH-ISOLATED MICROSTRIP ANTENNAS

Ref.	Single Patch	Inherent Isolation	20-dB Coupling Bandwidth*	Measured Efficiency	Antenna Height (λ_0)
[14]2023	No	Yes	7.2%	-	0.04
[25]2022	Yes	Yes	2.1%	> 83%	0.05
[27]2021	Yes	Yes	4.9%	70 - 86%	0.04
[29]2021	Yes	Yes	7.0%	> 92%	0.13
[31]2023	No	Yes	27.5%	82 – 93%	0.14
Proposed	Yes	Yes	22.2% / 19.8%	91 - 99%	0.18 / 0.12

*This is calculated under the condition that the S_{11} is better than -10 dB.

C. Comparison and Discussions

A comprehensive comparison is summarized in Table I. Although all these works can achieve inherent isolation without using any other decoupling structures, the decoupling bandwidth is lower than 8% in [14], [25], [27], and [29], somewhat not enough to support the wideband applications. The stacked patch scheme in [31] reached 27.5% decoupling bandwidth by using two patches but increasing the implementation difficulty and total cost. Although the design in [36] also shares the radiator, it is based on the mode cancellation principle, and the achieved 20 dB bandwidth is only about 6%. Although a coupling-fed structure, a ring slot, is also used in [29], it works for impedance matching enhancement. Differently, the proposed antenna achieves more than 22% decoupling bandwidth using only one radiating patch, providing a promising alternative for wideband IBFD antenna domain SIC.

IV. CONCLUSION

In this letter, a copolarized patch-shared wideband microstrip IBFD antenna is proposed. Two parallel-placed L-probes excite the same patch, forming an air-filled antenna pair that shares a single patch. There exist two coupling paths, the probe-probe one and the probe-patch-probe one, and the coupling coefficients of these two paths are analytically studied using the coupled resonators theory. It is found that the coupled energy from the two coupling paths is exactly counteracted, resulting in naturally high isolation between the two ports. Moreover, the employment of L-probes brings a wide bandwidth for the proposed antenna.

REFERENCES

[1] K. E. Kolodziej, B. T. Perry, and J. S. Herd, "In-band full-duplex technology: Techniques and systems survey," *IEEE Trans. Microw. Theory Techn.*, vol. 67, no. 7, pp. 3025–3041, Jul. 2019.

[2] Z. Zhang, K. Long, A. V. Vasilakos, and L. Hanzo, "Full-duplex wireless communications: Challenges, solutions, and future research directions," *Proc. IEEE*, vol. 104, no. 7, pp. 1369–1409, Jul. 2016.

[3] P. V. Prasannakumar, M. A. Elmansouri, and D. S. Filipovic, "Wideband decoupling techniques for dual-polarized bi-static simultaneous transmit and receive antenna subsystem," *IEEE Trans. Antennas Propag.*, vol. 65, no. 10, pp. 4991–5001, Oct. 2017.

[4] K. Kumari, M. Saikia, R. K. Jaiswal, S. Malik, and K. V. Srivastava, "A compact, low-profile shorted $TM_{1/2,0}$ mode planar copolarized microstrip antenna for full-duplex systems," *IEEE Antennas Wireless Propag. Lett.*, vol. 21, no. 9, pp. 1887–1891, Sep. 2022.

[5] A. Jafargholi, A. Jafargholi, and J. H. Choi, "Mutual coupling reduction in an array of patch antennas using CLL metamaterial superstrate for MIMO applications," *IEEE Trans. Antennas Propag.*, vol. 67, no. 1, pp. 179–189, Jan. 2019.

[6] T. Pei, L. Zhu, J. Wang, and W. Wu, "A low-profile decoupling structure for mutual coupling suppression in MIMO patch antenna," *IEEE Trans. Antennas Propag.*, vol. 69, no. 10, pp. 6145–6153, Oct. 2021.

[7] K. Iwamoto, M. Heino, K. Haneda, and H. Morikawa, "Design of an antenna decoupling structure for an inband full-duplex collinear dipole array," *IEEE Trans. Antennas Propag.*, vol. 66, no. 7, pp. 3763–3768, Jul. 2018.

[8] K.-L. Wu, C. Wei, X. Mei, and Z.-Y. Zhang, "Array-antenna decoupling surface," *IEEE Trans. Antennas Propag.*, vol. 65, no. 12, pp. 6728–6738, Dec. 2017.

[9] F. Liu, J. Guo, L. Zhao, G. Huang, Y. Li, and Y. Yin, "Dual-band metasurface-based decoupling method for two closely packed dual-band antennas," *IEEE Trans. Antennas Propag.*, vol. 68, no. 1, pp. 552–557, Jan. 2020.

[10] E. A. Etellisi, M. A. Elmansouri, and D. S. Filipovic, "Wideband monostatic co-polarized co-channel simultaneous transmit and receive broadside circular array antenna," *IEEE Trans. Antennas Propag.*, vol. 67, no. 2, pp. 843–852, Feb. 2019.

[11] D. Wu, Y. Zang, H. Luyen, M. Li, and N. Behdad, "A compact, low profile simultaneous transmit and receive antenna with monopole-like radiation characteristics," *IEEE Antennas Wireless Propag. Lett.*, vol. 18, no. 4, pp. 611–615, Apr. 2019.

[12] L. Sun, Y. Li, Z. Zhang, and Z. Feng, "Compact co-horizontally polarized full-duplex antenna with omnidirectional patterns," *IEEE Antennas Wireless Propag. Lett.*, vol. 18, no. 6, pp. 1154–1158, Jun. 2019.

[13] H. Lin, Q. Chen, Y. Ji, X. Yang, J. Wang, and L. Ge, "Weak-field-based self-decoupling patch antennas," *IEEE Trans. Antennas Propag.*, vol. 68, no. 6, pp. 4208–4217, Jun. 2020.

[14] Q. X. Lai, Y. M. Pan, and S. Y. Zheng, "A self-decoupling method for MIMO antenna array using characteristic mode of ground plane," *IEEE Trans. Antennas Propag.*, vol. 71, no. 3, pp. 2126–2135, Mar. 2023.

[15] Y.-F. Cheng and K.-K.-M. Cheng, "Decoupling of 2×2 MIMO antenna by using mixed radiation modes and novel patch element design," *IEEE Trans. Antennas Propag.*, vol. 69, no. 12, pp. 8204–8213, Dec. 2021.

[16] M. Li, S. Tian, M. Tang, and L. Zhu, "A compact low-profile hybrid-mode patch antenna with intrinsically combined self-decoupling and filtering properties," *IEEE Trans. Antennas Propag.*, vol. 70, no. 2, pp. 1511–1516, Feb. 2022.

[17] J. Wu, C. Tong, N. Yang, K. W. Leung, K. Lu, and P. Hu, "Radiation pattern decoupled patch antennas based on TM_{01} and TM_{11} modes," *IEEE Antennas Wireless Propag. Lett.*, vol. 22, no. 11, pp. 2695–2699, Nov. 2023.

[18] J. Sui and K.-L. Wu, "A self-decoupled antenna array using inductive and capacitive couplings cancellation," *IEEE Trans. Antennas Propag.*, vol. 68, no. 7, pp. 5289–5296, Jul. 2020.

[19] Y. Fang, L.-S. Wu, L.-F. Qiu, and Y. P. Zhang, "A method of introducing coupling null by shorting pins for stacked microstrip patch antenna array," *IEEE Trans. Antennas Propag.*, vol. 70, no. 7, pp. 6030–6035, Jul. 2022.

[20] L. Sun, Y. Li, and Z. Zhang, "Decoupling between extremely closely spaced patch antennas by mode cancellation method," *IEEE Trans. Antennas Propag.*, vol. 69, no. 6, pp. 3074–3083, Jun. 2021.

[21] J.-F. Qian, S. Gao, B. S. Izquierdo, H. Wang, H. Zhou, and H. Xu, "Mutual coupling suppression between two closely placed patch antennas using higher order modes," *IEEE Trans. Antennas Propag.*, vol. 71, no. 6, pp. 4686–4694, Jun. 2023.

[22] Y.-M. Zhang, S. Zhang, J.-L. Li, and G. F. Pedersen, "A dual-polarized linear antenna array with improved isolation using a slotline-based 180° hybrid for full-duplex applications," *IEEE Antennas Wireless Propag. Lett.*, vol. 18, no. 2, pp. 348–352, Feb. 2019.

[23] A. Afshani and K. Wu, "Dual-polarized patch antenna excited concurrently by a dual-mode substrate integrated waveguide," *IEEE Trans. Antennas Propag.*, vol. 70, no. 3, pp. 2322–2327, Mar. 2022.

[24] Q. Tan and K.-M. Luk, "Wideband co-linearly polarized magneto-electric dipole antenna for in-band full-duplex applications," *IEEE Trans. Antennas Propag.*, vol. 71, no. 2, pp. 1907–1912, Feb. 2023.

[25] A. Zhang, K. Wei, Y. Hu, and Q. Guan, "High-isolated coupling-grounded patch antenna pair with shared radiator for the application of 5G mobile terminals," *IEEE Trans. Antennas Propag.*, vol. 70, no. 9, pp. 7896–7904, Sep. 2022.

[26] J. Hu, W. Zhang, Y. Li, and Z. Zhang, "Compact co-polarized PIFAs for full-duplex application based on CM/DM cancellation theory," *IEEE Trans. Antennas Propag.*, vol. 69, no. 11, pp. 7103–7110, Nov. 2021.

[27] Y. He and Y. Li, "Compact co-linearly polarized microstrip antenna with fence-strip resonator loading for in-band full-duplex systems," *IEEE Trans. Antennas Propag.*, vol. 69, no. 11, pp. 7125–7133, Nov. 2021.

[28] Z. Wan, Y. He, Y. Bai, and H. Sun, "Compact, copolarized, and high-isolation two-port patch antenna for MIMO applications," *IEEE Antennas Wireless Propag. Lett.*, vol. 22, no. 11, pp. 2705–2709, Nov. 2023.

[29] K.-L. Wong, M.-F. Jian, C.-J. Chen, and J.-Z. Chen, "Two-port same-polarized patch antenna based on two out-of-phase TM_{10} modes for access-point MIMO antenna application," *IEEE Antennas Wireless Propag. Lett.*, vol. 20, no. 4, pp. 572–576, Apr. 2021.

[30] N.-W. Liu, B.-B. Huang, L. Zhu, and G. Fu, "Low-profile four-port patch antenna with wide isolation bandwidth and same polarization: Principle and design approach," *IEEE Antennas Wireless Propag. Lett.*, vol. 22, no. 10, pp. 2407–2411, Oct. 2023.

[31] Y.-Z. Liang, F.-C. Chen, K.-R. Xiang, and W.-F. Zeng, "Wideband co-polarized stacked patch antenna for in-band full-duplex applications," *IEEE Trans. Antennas Propag.*, vol. 71, no. 12, pp. 9920–9925, Dec. 2023.

[32] C. L. Mak, K. M. Luk, K. F. Lee, and Y. L. Chow, "Experimental study of a microstrip patch antenna with an L-shaped probe," *IEEE Trans. Antennas Propag.*, vol. 48, no. 5, pp. 777–783, May 2000.

[33] H. Wong, K. L. Lau, and K. M. Luk, "Design of dual-polarized L-probe patch antenna arrays with high isolation," *IEEE Trans. Antennas Propag.*, vol. 52, no. 1, pp. 45–52, Jan. 2004.

[34] R. J. Cameron, C. M. Kudsia, and R. R. Mansour, *Microwave Filters for Communication Systems: Fundamentals, Design and Applications*. New York, NY, USA: Wiley, 2007.

[35] H. Meng and K.-L. Wu, "Direct optimal synthesis of a microwave bandpass filter with general loading effect," *IEEE Trans. Microw. Theory Techn.*, vol. 61, no. 7, pp. 2566–2573, Jul. 2013.

[36] L. Sun, Y. Li, Z. Zhang, and H. Wang, "Self-decoupled MIMO antenna pair with shared radiator for 5G smartphones," *IEEE Trans. Antennas Propag.*, vol. 68, no. 5, pp. 3423–3432, May 2020.